

Article

Microbial Transformation of Galangin Derivatives and Cytotoxicity Evaluation of Their Metabolites

Fubo Han, Yina Xiao and Ik-Soo Lee *

College of Pharmacy and Research Institute of Pharmaceutical Sciences, Chonnam National University, Gwangju 61186, Korea; hanfubo0306@gmail.com (F.H.); yogurtxiao@163.com (Y.X.)

* Correspondence: islee@chonnam.ac.kr; Tel.: +82-62-530-2932

Abstract: Galangin (1), 3-*O*-methylgalangin (2), and galangin flavanone (3), the major bioactive flavonoids isolated from *Alpinia officinarum*, were biotransformed into one novel and four known metabolites (4–8) by application of the fungal strains *Mucor hiemalis* and *Absidia coerulea* as biocatalysts. Their structures were characterized by extensive spectroscopic analyses including one- and two-dimensional nuclear magnetic resonance spectroscopy and mass spectrometry. Compounds 1–7 were evaluated for their cytotoxic activities against cancer cell lines using the MTT assay. The new compound 3-*O*-methylgalangin-7-*O*- β -D-glucopyranoside (6) exhibited the most potent cytotoxic activity against MCF-7, A375P, B16F10, B16F1, and A549 cancer cell lines with the IC₅₀ values at 3.55–6.23 μ M.

Keywords: *Alpinia officinarum*; galangin; microbial transformation; cytotoxic activity



Citation: Han, F.; Xiao, Y.; Lee, I.-S. Microbial Transformation of Galangin Derivatives and Cytotoxicity Evaluation of Their Metabolites. *Catalysts* **2021**, *11*, 1020. <https://doi.org/10.3390/catal11091020>

Academic Editors: Katarzyna Wińska, Wanda Mączka and Antoni Szumny

Received: 3 June 2021

Accepted: 21 August 2021

Published: 24 August 2021

Publisher's Note: MDPI stays neutral with regard to jurisdictional claims in published maps and institutional affiliations.



Copyright: © 2021 by the authors. Licensee MDPI, Basel, Switzerland. This article is an open access article distributed under the terms and conditions of the Creative Commons Attribution (CC BY) license (<https://creativecommons.org/licenses/by/4.0/>).

1. Introduction

The rhizome of *Alpinia officinarum* Hance (AOH), commonly known as lesser galangal, is a well-known traditional Chinese medicine that has been widely used as an antiemetic, stomachic, and analgesic in Asia for thousands of years [1,2]. The anticancer potential of AOH has been attracting keen interest from the scientific community. It has been reported to produce anticancer effects against a wide variety of human cancers including melanoma, liver, colon, breast, and lung cancers [3]. The growing body of evidence suggests that AOH contains potent anti-proliferative agents and may serve as a basis for anticancer drugs in the future.

Flavonoids have been reported to demonstrate promising results when used against different tumor cell lines, including melanoma cells [4]. Furthermore, flavonoids naturally exhibit low toxicity in biological systems, which makes them an alternative therapy for the treatment of cancers in comparison with traditional anticancer drugs [5]. Flavonoids of AOH have been reported to exhibit various pharmacological effects such as analgesic, antiemetic, antioxidant, hypoglycemic, and anticancer activities [6] consistent with the functions and indications of AOH, indicating that flavonoids are the basic medicinal components of AOH.

In Chinese Pharmacopoeia, galangin (1) is the only marker compound for the quality control of AOH [7]. It also appears to be the predominant constituent in all parts of AOH with antioxidant, antiobesogenic, and anti-inflammatory properties [8]. Furthermore, recent research has shown that galangin has anticancer effects against various cancers including hepatocellular carcinoma, breast cancer, lung cancer, gastric cancer, cervical cancer, and melanoma [9–11]. In addition, the results have demonstrated that the effects of galangin were selective for cancer cells and did not lead to any cytotoxicity against normal cells [9].

Pinocebrin (3), also known as galangin flavanone, is a pharmacologically active flavonoid that can be isolated from propolis and a variety of medicinal plants, such as *Alpinia officinarum*, *Alpinia katsumadai*, and *Glycyrrhiza glabra* L. [8,12,13]. It was shown

to exhibit anti-inflammatory, antioxidant, and neuroprotective activities and has been approved by China Food and Drug Administration (CFDA) as a new drug for the treatment of ischemic stroke [13,14]. Recent pharmacological studies revealed that it possesses antitumor effects, such as against melanoma cells [15].

Glycosylation is an important modification strategy that has been commonly used to obtain flavonoid glycosides that are not encountered among natural analogues [16]. The addition of glycosidic moieties or glycosylation makes the flavonoid less reactive and more polar, leading to more water solubility [17]. In a metal-catalyzed oxidative degradation study of the glycoside rutin and its aglycone quercetin, it was found that rutin had a slower degradation rate than quercetin [18]. Moreover, flavonoid *O*-glycosides have been proven to have promising pharmaceutical effects [19]. Thus, more interest has been drawn to the isolation and pharmacological study of these types of compounds. Though many well-designed chemical glycosylation methods are available, it is not easy to accomplish regioselective glycosylation since it is often hampered by the presence of various hydroxyl groups in the glycosylation acceptors (i.e., aglycones) [20,21]. It is often required that these hydroxyl groups be selectively protected and deprotected to avoid by-product formation in the glycosylation process [21,22]. For instance, the hydroxyl groups of the glycosylation acceptors baicalein and quercetin were selectively protected and deprotected during the synthesis of their corresponding 7-*O*-glycosides [23,24]. Microbial transformation can be used as an efficient method for producing these types of compounds, since in a majority of cases it does not require the protection of existing functional groups. In addition, it is carried out under mild conditions and has a number of advantages over chemical synthesis such as higher stereo- and regio-selectivity [25,26].

It has been reported that glucosylation of flavonoids can be performed by several fungal strains, such as *Absidia coerulea*, *Cunninghamella echinulata*, *Cunninghamella elegans*, and *Mucor hiemalis* [26,27]. During this investigation, *M. hiemalis* was used to transform galangin and its derivatives (1–3) and scale-up fermentation led to the isolation of one novel and three known glucosylated metabolites (4–7, Figure 1). All of the compounds were evaluated for cytotoxic activities against cancer cell lines MCF-7 (human breast cancer cells), A375P (human melanoma cells), B16F1 and B16F10 (murine melanoma cells), and A549 (human lung cancer cells) by using the MTT assay, and it was revealed that 3-*O*-methylgalangin-7-*O*- β -D-glucopyranoside (6) has the strongest activity among all the tested compounds with IC_{50} values at 3.55–6.23 μ M.

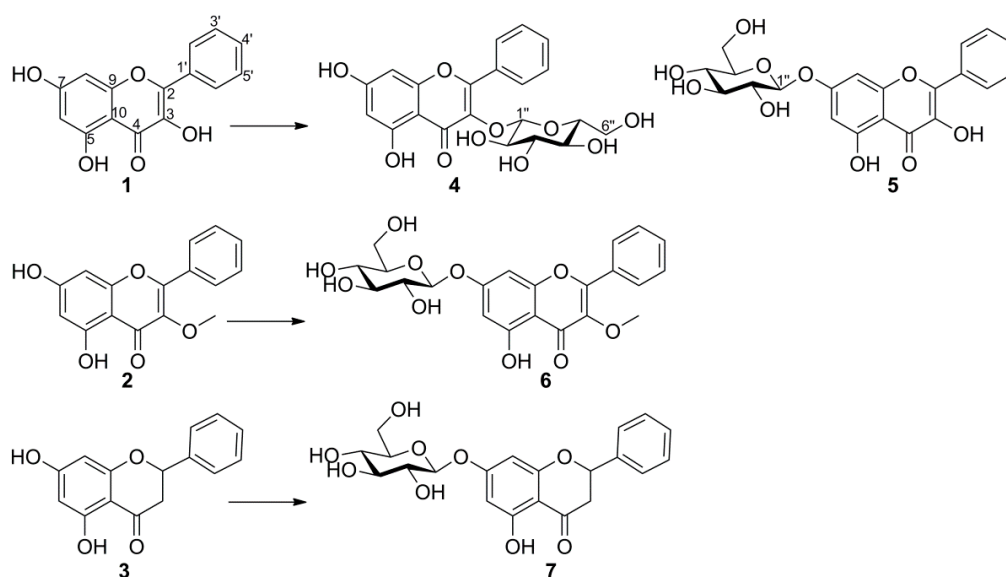


Figure 1. Microbial transformation of compounds 1–3 by *M. hiemalis*.

2. Results and Discussion

Galangin (**1**) and its derivatives 3-*O*-methylgalangin (**2**) and galangin flavanone (pinocembrin, **3**) were isolated from *Alpinia officinarum* by column chromatographic methods and identified by comparison of their NMR data with those reported in the literature and retention times with standard compounds. Of the 14 microorganisms screened, *Mucor hiemalis* KCTC 26779 and *Absidia coerulea* KCTC 6936 were selected for preparative-scale fermentation studies since they were found to be capable of metabolizing **1–3** based on the analysis of TLC plates involving the substrate and culture controls. Scale-up fermentation with *M. hiemalis* and *A. coerulea* led to the isolation of one novel and four known metabolites and their chemical structures were identified as galangin-3-*O*- β -D-glucopyranoside (**4**), galangin-7-*O*- β -D-glucopyranoside (**5**), 3-*O*-methylgalangin-7-*O*- β -D-glucopyranoside (**6**), pinocembrin-7-*O*- β -D-glucopyranoside (**7**), and galangin-7-*O*-sulfate (**8**) based on the spectroscopic analyses.

2.1. Identification of Metabolites

The compound **4** was obtained as a yellow solid. A HRESIMS spectrum of **4** exhibited a $[M+Na]^+$ peak at m/z 455.0953, which established a molecular formula of $C_{21}H_{20}O_{10}Na$, suggesting that it was a glycosylated metabolite of **1**. The coupling constant of the anomeric proton signal at δ_H 5.49 was in the range of 7–8 Hz, suggesting the sugar unit has a β -linkage. The sugar was obtained after acid hydrolysis of **4** and was identified as D-glucose based on the ^{13}C -NMR spectrum and TLC comparison with the authentic sample (Figure S2). Lipkind and colleagues reported that different monosaccharides show different ^{13}C -NMR spectra [28]. The presence of D-glucose moiety was further confirmed by comparison of the carbon signals of **4** with those of D-galactose, D-fructose, and D-mannose moieties in the literature [29–32]. The proton signals at δ_H 12.50 (s, 5-OH), 8.11 (m, H-2'/6'), 7.55 (m, H-3'/4'/5'), 6.47 (d, $J = 1.5$ Hz, H-8), and 6.25 (d, $J = 1.5$ Hz, H-6) were similar to those of compound **1**, which indicated that the sugar moiety was attached at the C-3 position of the aglycone through an ether linkage. The crucial heteronuclear multiple-bond correlation (HMBC) between H-1'' and C-3 further confirmed the attachment of glucose moiety at C-3 position (Figure 2). After comparison with previously reported data [27,33], the structure of **4** was elucidated as galangin-3-*O*- β -D-glucopyranoside.

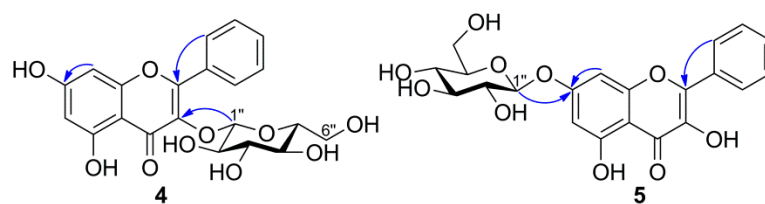


Figure 2. Key HMBC correlations ($^1H \rightarrow ^{13}C$) of compounds **4** and **5**.

The compound **5** was obtained as a pale yellow solid. A HRESIMS spectrum of **5** exhibited a $[M+Na]^+$ peak at m/z 455.0954, suggesting that the molecular formula of **5** was $C_{21}H_{20}O_{10}$, which was one glucose unit higher than that of **1**. 1H -NMR data of **5** was quite similar to that of **4**, showing characteristic resonances of galangin and a D-glucose moiety. The proton signals of **5** at δ_H 6.84 (1H, $J = 2.2$ Hz, d, H-8) and 6.45 (1H, $J = 2.2$ Hz, H-6) were significantly downfield-shifted compared with **1**, which indicated that the glucose moiety was attached to C-7. In addition, the C-7 substitution was further supported by the HMBC correlation from the anomeric proton signal at δ_H 5.09 to the carbon signal at δ_C 163.5 (Figure 2). After comparison with previously reported data of chrysin-7-*O*-glucoside and kaempferol-7-*O*-glucoside [34,35], the structure of **5** was elucidated as galangin-7-*O*- β -D-glucopyranoside.

The compound **6** was obtained as a white solid. A HRESIMS spectrum of **6** exhibited a sodiated molecule at m/z 469.1112 and a peak at m/z 285.0768 ($[M+H-162]^+$), suggesting the presence of one sugar moiety. The sugar obtained from acid hydrolysis of **6** was

identified as D-glucose based on the TLC comparison with the authentic sample. ^1H - and ^{13}C -NMR spectra confirmed the presence of 3-O-methylgalangin and a glucose moiety in the structure. The presence of a 3-O-methylgalangin skeleton was deduced from a hydroxyl proton at δ_{H} 12.56 (s, 5-OH), two doublet protons at δ_{H} 6.48 (d, $J = 2.1$ Hz, H-6), and 6.83 (d, $J = 2.1$ Hz, H-8) on the A-ring, one set of $\text{A}_2\text{B}_2\text{X}$ type aromatic protons at δ_{H} 8.03 (m, H-2'/6') and 7.61 (m, H-3'/4'/5') on the B-ring, and, together with a methoxyl proton at δ_{H} 3.83 (s, 3-OCH₃), on the C-ring. Furthermore, the anomeric signals of the glycosidic linkage at δ_{H} 5.09 (d, $J = 7.1$ Hz, H-1'') and δ_{C} 100.3 (C-1'') were evident in the ^1H - and ^{13}C -NMR spectra. The multiplet signals at δ_{H} 3.27–3.47 (5H, m, H-2''–H-6'') and 3.71 (dd, H-6'') were assignable to the methine and methylene protons of the glucose moiety. The signals at δ_{H} 5.42 (d, 2''-OH), 5.14 (d, 3''-OH), 5.08 (d, 4''-OH), and 4.62 (t, 6''-OH) were assigned as the hydroxyl protons of the glucose unit.

The HMBC spectrum of **6** showed a correlation from the anomeric proton (H-1'') of the glucose moiety to the C-7 on the A-ring of the aglycone, suggesting the attachment of the sugar unit to the 7-OH group (Figure 3). Also, the glycosidic linkage at C-7 of the aglycone was viewed from the upfield-shift of δ_{C} 163.6 (C-7) as compared with **2**. The large coupling constant of the anomeric proton H-1'' (7.1 Hz) indicated the configuration of glucose moiety is in β -form. Therefore, the structure of compound **6** was elucidated as 3-O-methylgalangin-7-O- β -D-glucopyranoside.

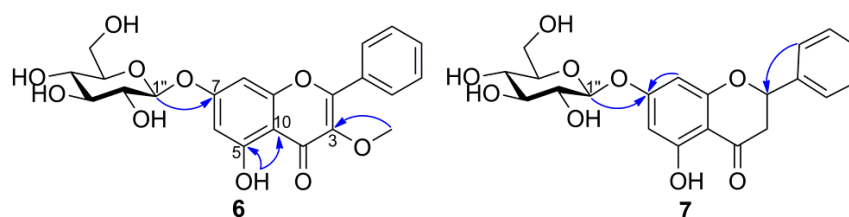


Figure 3. Key HMBC correlations ($^1\text{H} \rightarrow ^{13}\text{C}$) of compounds **6** and **7**.

The compound **7** was obtained as a white solid. A HRESIMS spectrum of **7** exhibited a $[\text{M}+\text{Na}]^+$ peak at m/z 441.1162, suggesting the molecular formula of **7** to be $\text{C}_{21}\text{H}_{22}\text{O}_9$, which was one glucose unit higher than that of **3**. The ^1H -NMR spectrum of **7** showed a series of signals between δ_{H} 3.70–3.10 together with the downfield-shifted signals at δ_{H} 6.20 (H-8) and 6.15 (H-6), which are attributable to a sugar moiety substituted at C-7 position through an ether linkage. The coupling constant of the anomeric proton ($J = 7.4$ Hz) at δ_{H} 4.98 and the ^{13}C -NMR chemical shifts of the sugar carbons (δ_{C} 100.1, 79.1, 76.8, 73.5, 70.0, and 61.1) revealed the presence of a β -D-glucose unit in **7**. Upon further comparison with previously reported data [36], the structure of **7** was elucidated as pinocembrin-7-O- β -D-glucopyranoside.

The compound **8** was obtained as a yellow amorphous powder. A HRESIMS spectrum of **8** exhibited a peak of the protonated molecule at m/z 351.0448, which is 80 mass units higher than that of galangin (**1**), suggesting the presence of a sulfate group. This was confirmed using the acid hydrolysis method [37,38], which resulted in a white precipitate of the aqueous layer after treating with BaCl_2 . Meanwhile, the strong bands at 1257 cm^{-1} (S=O) and 1023 cm^{-1} (C–O–S) in the IR spectrum further supported the presence of sulfate moiety [38]. NMR spectroscopy was used to identify the attachment site of the sulfate group [39–41]. Comparison of the ^1H - and ^{13}C -NMR data of **8** with those of galangin [42] revealed the significant changes of resonance signals in ring A. The downfield-shifts of H-6, H-8, C-6, C-8, and C-10 (0.41, 0.63, 3.6, 4.4, and 2.2 ppm, respectively) and upfield-shift of C-7 (4.1 ppm) implied that the sulfate moiety was conjugated with 7-OH (Figure 4). Hence, the structure of **8** was assigned galangin-7-O-sulfate.

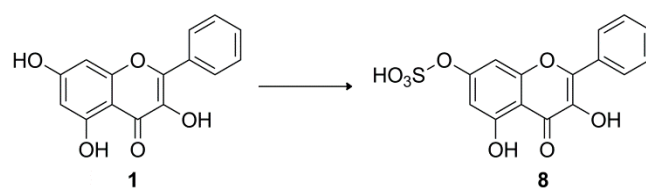


Figure 4. Microbial transformation of compound **1** by *A. coerulea*.

2.2. Cytotoxic Activity

Despite the various biological activity studies of galangin and its derivatives that have been undertaken, investigations have rarely been conducted on their glucosylated metabolites. In this study, compounds **1–7** were evaluated for their in vitro cytotoxic activities against MCF-7, A375P, B16F10, B16F1, and A549 cancer cell lines using the MTT assay (Table 1). All of the 7-*O*-glucosylated metabolites (**5–7**) exhibited activities against the tested cells, and among them, metabolites **5** (IC₅₀ 5.47–30.43 μM) and **6** (IC₅₀ 3.55–6.23 μM) showed more potent activity than their parent compounds **1** (IC₅₀ 61.06–84.74 μM) and **2** (IC₅₀ ≥100 μM), respectively. Goodarzi and colleagues reported that luteolin-7-*O*-glucoside showed stronger cytotoxic activity than its aglycone luteolin against the breast cancer cell line MCF-7 (IC₅₀: 3.98 μg/mL and 32.86 μg/mL, respectively) [43]. Smiljkovic and colleagues reported that apigenin-7-*O*-glucoside exhibited stronger cytotoxic activity than its aglycone apigenin against the colon cancer cell HCT116 (IC₅₀: 15 μM and 62 μM, respectively) [44]. Ikemoto and colleagues observed that baicalin (baicalein-7-*O*-glucuronide) exhibited much stronger cytotoxic activities than baicalein against the bladder cancer cell lines KU-1 and EJ-1, and comparable effects against MBT-2 cells [45]. Aisyah et al. observed that the 3-*O*-glycosylated metabolites of kaempferol and quercetin showed much weaker cytotoxic activities than their aglycones kaempferol and quercetin against the murine leukemia cell P-388 [46]. These results suggested that *O*-glycosylation of flavonoids at the C-7 position could enhance their cytotoxic activities.

Table 1. Cytotoxic activities of compounds **1–7** against cancer cell lines.

Compounds	Cell Lines (IC ₅₀ , μM)				
	MCF-7	A375P	B16F10	B16F1	A549
1	79.44 ± 2.53	84.74 ± 1.70	61.06 ± 2.50	62.46 ± 4.81	63.64 ± 6.24
2	99.83 ± 4.13	>100	>100	>100	>100
3	66.56 ± 0.45	55.35 ± 0.85	24.02 ± 0.77	30.15 ± 1.85	48.33 ± 1.56
4	>100	>100	>100	>100	>100
5	5.47 ± 2.16	30.43 ± 0.69	12.65 ± 0.74	28.65 ± 2.75	6.30 ± 0.34
6	3.55 ± 0.49	6.23 ± 1.95	4.38 ± 0.06	3.75 ± 0.25	4.83 ± 0.90
7	104.30 ± 2.70	110.60 ± 1.50	62.43 ± 1.79	80.62 ± 5.46	39.34 ± 1.89
DZ ¹	5.12 ± 0.44	9.86 ± 0.57	6.61 ± 0.83	5.42 ± 0.46	4.01 ± 0.78

¹ Used as positive control.

Transmembrane delivery of flavonoid glycosides was reported to be carried out by glycoside binding to glucose transporters on the cell membrane [47]. Sodium-glucose cotransporter 1 and glucose transporter 2 mediated the cross-membrane transport of quercetin-3-*O*-glucoside and cyanidin-3-*O*-glucoside in Caco-2 cells [48]. In addition, due to competition for the glucose transporter, the absorption of cyanidin-3-*O*-glucoside was inhibited by quercetin-3-*O*-glucoside [49]. The glucose transporters are widely expressed in cancer cells including breast cancer, melanoma, and lung cancer cells [50–52]. Thus, the glucosylated compounds might exhibit cytotoxic activity against the tested cancer cells via entering the cellular compartment through glucose transporters.

Some results indicated that flavonoid glycosides had similar or even better bioactivities compared to their aglycones when applied in vivo [53]. In our opinion, the concern of how various flavonoid glycosides influence the biological activity in vivo could be the subject of further investigation [54].

3. Materials and Methods

3.1. General Experimental Procedures

The 1D- and 2D-NMR spectra were recorded in DMSO- d_6 on a Bruker Avance III HD 400 spectrometer (Bruker, Billerica, MA, USA), using TMS as the internal standard. The chemical shift values (δ) are reported in ppm units, and the coupling constants (J) are in Hz. Melting points were determined on a DigiMelt MPA 160 melting point apparatus (Stanford Research Systems, Sunnyvale, CA, USA) and a Thomas-Hoover Uni-Melt capillary melting point apparatus (Thomas Scientific, Swedesboro, NJ, USA). UV spectra were taken with a JASCO V-530 spectrophotometer (Jasco, Tokyo, Japan). IR spectra were obtained on a PerkinElmer Spectrum 400 FT-IR and FT-NIR spectrometer (Waltham, MA, USA). High resolution electrospray ionization mass spectrometry (HRESIMS) analysis was recorded on a Synapt G2 mass spectrometer (Waters, Milford, MA, USA). Separation and purification were carried out by column chromatography on silica gel (70~230 mesh). Thin layer chromatography (TLC) was performed on precoated silica gel 60 F₂₅₄ plates (Merck, Darmstadt, Germany) using chloroform:methanol (5:1, v/v) solution. TLC plates were visualized under UV light (254 and 365 nm) and by heating the plates sprayed with anisaldehyde-H₂SO₄ reagent. High-performance liquid chromatography (HPLC) was performed on a Waters 1525 Binary HPLC pump connected to a Waters 996 Photodiode Array detector (Waters Corp., Milford, MA, USA) using a Phenomenex Luna C18 (250 × 10 mm, 5 μ m) column with the solvent system of methanol and water at a flow rate of 2.0 mL/min. All the chemicals and solvents used for the extraction and isolation were of analytical grade.

3.2. Materials and Microorganisms

The rhizomes of *Alpinia officinarum* Hance were purchased from Sehwadang (Gwangju, Korea), which was identified by DaeHyo Pharmacy Co., Ltd. (Suwon, Korea), and a voucher specimen (KDALP1901) has been deposited at College of Pharmacy, Chonnam National University. Galangin and its derivatives (1–3) were isolated from *A. officinarum* and confirmed by NMR in comparison with the standard compounds purchased from Biopurify Phytochemicals Ltd. (Chengdu, China). Briefly, the powder of *A. officinarum* was extracted with MeOH under sonication and partitioned with hexane, dichloromethane (CH₂Cl₂), ethyl acetate (EtOAc), and water. The EtOAc extract was subjected to column chromatography, using CH₂Cl₂:MeOH to give 14 fractions. The flavonoid-rich fraction 4 was dissolved in MeOH, separated using HPLC method to give compounds 1–3.

3.2.1. Galangin (1)

Yellow solid. mp. 214–215 °C (ref: 213.5–215 °C [42]). ¹H-NMR (DMSO- d_6 , 400 MHz) δ 6.18 (1H, d, J = 2.1 Hz, H-6), 6.39 (1H, d, J = 2.1 Hz, H-8), 7.38–7.52 (3H, m, H-3'/4'/5'), 8.12–8.20 (2H, m, H-2'/6'). (Supplementary Materials, Figure S4).

3.2.2. 3-O-Methylgalangin (2)

Pale yellow solid. mp. 282–283 °C (ref: 286–287 °C [55]). ¹H-NMR (DMSO- d_6 , 400 MHz) δ 12.57 (1H, s, 5-OH), 6.22 (1H, d, J = 1.5 Hz, H-6), 6.46 (1H, d, J = 1.5 Hz, H-8), 7.59 (3H, m, H-3'/4'/5'), 8.00 (2H, m, H-2'/6'), 3.81 (3H, s, 3-OCH₃). (Supplementary Materials, Figure S5).

3.2.3. Pinocembrin (3)

White solid. mp. 193–194 °C (ref: 191–193 °C [55]). ¹H-NMR (DMSO- d_6 , 400 MHz) δ 5.44 (1H, dd, J = 3.1, 12.7 Hz, H-2), 3.07 (1H, dd, J = 12.7, 17.1 Hz, H-3a), 2.76 (1H, dd, J = 3.1, 17.1 Hz, H-3b), 5.90 (1H, d, J = 2.2 Hz, H-6), 5.93 (1H, d, J = 2.2 Hz, H-8), 7.33–7.43 (3H, m, H-3'/4'/5'), 7.45–7.51 (2H, m, H-2'/6'). (Supplementary Materials, Figure S6).

The microorganisms were obtained from the Korean Collection for Type Cultures (KCTC) at the Korea Research Institute of Bioscience and Biotechnology (KRIBB), Daejeon, Korea. The cultures used for preliminary screening are listed below: *Absidia coerulea* 6936, *Alternaria alternata* 6005, *Aspergillus fumigatus* 6145, *Candida famata* 7000, *Cunninghamella*

elegans var. *elegans* 6992, *Glomeralla cingulata* 6075, *Hormoconis resiniae* 6966, *Metschnikowia pulcherrima* 7605, *Mortierella remanniana* var. *angulispora* 6137, *Mucor hiemalis* 26779, *Penicillium chrysogenum* 6933, *Pichia pastoris* 7190, *Trichoderma koningii* 6042, and *Tremella mesenterica* 7131. *A. fumigatus*, *M. hiemalis* and *P. chrysogenum* were cultured on a malt medium (malt extract 20 g/L, D-glucose 20 g/L, peptone 1 g/L); *C. elegans* var. *elegans* and *H. resiniae* were cultured on a potato dextrose medium (24 g/L); other microorganisms were cultured on yeast-malt medium (D-glucose 10 g/L, peptone 5 g/L, malt extract 3 g/L, and yeast extract 3 g/L). All of the ingredients for microbial growth media, including D-glucose, peptone, and malt extract were purchased from Becton, Dickinson and Company (Sparks, MD, USA). Demethylzeylasteral (DZ) used as control in the bioassay was purchased from Biopurify Phytochemicals Ltd. (Chengdu, China). Dulbecco's modified Eagle medium (DMEM) and Antibiotic-Antimycotic were purchased from Gibco (Invitrogen, Carlsbad, CA, USA). Fetal bovine serum (FBS) was purchased from Welgene Inc. (Gyeongsan-si, Korea). Phosphate buffered saline (PBS) tablets was purchased from Takara Korea Biomedical Inc. (Seoul, Korea), and thiazolyl blue tetrazolium bromide (MTT) was from Thermo Fisher Scientific (Waltham, MA, USA).

3.3. Microbial Screening Procedures

Microbial transformation studies were carried out according to a two-stage procedure [27]. Briefly, the actively growing microbial cultures were incubated in the 250 mL culture flasks containing 50 mL of the sterilized culture medium at 25 °C in a temperature-controlled shaking incubator (200 rpm). 2 mL inoculum derived from the first-stage culture was transferred to a fresh medium and incubated under the same condition for 24 h. The dimethyl sulfoxide (DMSO) solutions (1 mg/100 µL) of compounds 1–3 were then added to each flask at a concentration of 40 µg/mL and further incubated at the same conditions for another 5 days. General sampling and TLC monitoring were performed at intervals of 24 h. Substrate controls consisted of compounds 1–3 and sterilized culture media, and culture controls consisted of fermentation cultures in which the microorganisms were grown without addition of parent compounds.

3.4. Biotransformation of 1–3 by *M. Hiemalis* KCTC 26779

Scale-up fermentations were performed with four 500 mL culture flasks, each containing 125 mL malt media under the same conditions, and 40 mg of galangin (1, 0.148 mmol) dissolved in DMSO was evenly distributed between flasks. After incubation for five days, the microbial cultures were extracted with EtOAc (600 mL × 3), and the EtOAc layers were combined and concentrated under vacuum to yield a crude extract (272 mg). The EtOAc extract of 1 was dissolved in methanol and chromatographed on a semi-preparative reversed-phase HPLC with 60% MeOH as mobile phase to give metabolites 4 (9.36 mg, 15%) and 5 (53.65 mg, 84%). A similar scale-up process was performed for compounds 2 (10 mg, 0.035 mmol) and 3 (30 mg, 0.117 mmol), and the crude extracts (111 mg and 163 mg, respectively) were obtained after incubation for five days. The EtOAc extracts of compounds 2 and 3 were dissolved in methanol and then chromatographed on a semi-preparative reversed-phase HPLC with 60% MeOH as mobile phase to give metabolites 6 (4.56 mg, 30%) and 7 (46.34 mg, 95%), respectively.

3.4.1. Galangin-3-O-β-D-glucopyranoside (4)

Yellow solid. mp. 231–232 °C (ref: 218–220 °C [33]). IR (KBr) ν_{\max} cm⁻¹: 3321, 2926, 1655, 1609, 1363, 1210, 1179, 1073. UV (MeOH) λ_{\max} : 265 (3.09), 309 (1.34), 341 (1.18) nm. ¹H-NMR (DMSO-*d*₆, 400 MHz) δ 12.50 (1H, s, 5-OH), 6.25 (1H, d, *J* = 1.5 Hz, H-6), 6.47 (1H, d, *J* = 1.5 Hz, H-8), 7.55 (3H, m, H-3'/4'/5'), 8.11 (2H, m, H-2'/6'), 5.49 (1H, d, *J* = 7.6 Hz, H-1''), 3.15 (1H, m, H-2''), 3.24 (1H, m, H-3''), 3.09 (1H, m, H-4''), 3.11 (1H, m, H-5''), 3.59 (1H, m, H-6''a), 3.35 (1H, dd, *J* = 5.2, 11.3 Hz, H-6''b), 5.34 (1H, br s, 2''-OH), 5.03 (2H, br s, 3''/4''-OH), 4.31 (1H, br s, 6''-OH). ¹³C-NMR (DMSO-*d*₆, 100 MHz) δ 156.4 (C-2), 134.6 (C-3), 178.2 (C-4), 161.8 (C-5), 99.3 (C-6), 164.9 (C-7), 94.3 (C-8), 157.1(C-9), 104.7 (C-10),

130.9 (C-1'), 129.4 (C-2'/6'), 128.7 (C-3'/5'), 131.3 (C-4'), 101.1 (C-1''), 74.6 (C-2''), 76.8 (C-3''), 70.3 (C-4''), 78.0 (C-5''), 61.3 (C-6''). HRESIMS m/z 455.0953 [M+Na]⁺ (calcd for C₂₁H₂₀O₁₀Na, 455.0954). (Supplementary Materials, Figures S9–S14).

3.4.2. Galangin-7-O-β-D-glucopyranoside (5)

Pale yellow solid. mp. 246–247 °C. IR (KBr) ν_{\max} cm⁻¹: 3380, 2924, 2856, 1654, 1598, 1497, 1175, 1073. UV (MeOH) λ_{\max} : 265 (2.30), 309 (1.17), 359 (1.42) nm. ¹H-NMR (DMSO-*d*₆, 400 MHz) δ 12.36 (1H, s, 5-OH), 9.82 (1H, s, 3-OH), 6.45 (1H, *J* = 2.2 Hz, H-6), 6.84 (1H, *J* = 2.2 Hz, H-8), 7.55 (3H, m, H-3'/4'/5'), 8.17 (2H, m, H-2'/6'), 5.09 (1H, d, *J* = 7.4 Hz, H-1''), 3.28 (1H, m, H-2''), 3.31 (1H, m, H-3''), 3.18 (1H, m, H-4''), 3.47 (1H, m, H-5''), 3.72 (1H, dd, *J* = 5.1, 10.2 Hz, H-6''a), 3.49 (1H, m, H-6''b), 5.40 (1H, d, *J* = 4.8 Hz, 2''-OH), 5.12 (1H, d, *J* = 4.7 Hz, 3''-OH), 5.06 (1H, d, *J* = 5.2 Hz, 4''-OH), 4.61 (1H, t, *J* = 5.1 Hz, 6''-OH). ¹³C-NMR (DMSO-*d*₆, 100 MHz) δ 146.9 (C-2), 137.9 (C-3), 177.0 (C-4), 160.9 (C-5), 99.4 (C-6), 163.5 (C-7), 95.0 (C-8), 156.5 (C-9), 105.4 (C-10), 131.3 (C-1'), 128.1 (C-2'/6'), 129.0 (C-3'/5'), 130.6 (C-4'), 100.4 (C-1''), 73.6 (C-2''), 76.9 (C-3''), 70.0 (C-4''), 77.6 (C-5''), 61.1 (C-6''). HRESIMS m/z 455.0954 [M+Na]⁺ (calcd for C₂₁H₂₀O₁₀Na, 455.0954). (Supplementary Materials, Figures S15–S20).

3.4.3. 3-O-methylgalangin-7-O-β-D-glucopyranoside (6)

White solid. mp. 228–229 °C. IR (KBr) ν_{\max} cm⁻¹: 3275, 2927, 1653, 1610, 1183, 1099, 815. UV (MeOH) λ_{\max} : 265 (2.04), 303 (1.00), 340 (0.79) nm. ¹H-NMR (DMSO-*d*₆, 400 MHz) δ 12.56 (1H, s, 5-OH), 6.48 (1H, d, *J* = 2.1 Hz, H-6), 6.83 (1H, d, *J* = 2.1 Hz, H-8), 7.61 (3H, m, H-3'/4'/5'), 8.03 (2H, m, H-2'/6'), 5.09 (1H, d, *J* = 7.1 Hz, H-1''), 3.27 (1H, m, H-2''), 3.29 (1H, m, H-3''), 3.18 (1H, m, H-4''), 3.46 (1H, m, H-5''), 3.71 (1H, dd, *J* = 4.9, 9.8 Hz, H-6''a), 3.48 (1H, m, H-6''b), 5.42 (1H, d, *J* = 4.6 Hz, 2''-OH), 5.14 (1H, d, *J* = 4.4 Hz, 3''-OH), 5.08 (1H, d, *J* = 4.0 Hz, 4''-OH), 4.62 (1H, t, *J* = 5.2 Hz, 6''-OH), 3.83 (3H, s, 3-OCH₃). ¹³C-NMR (DMSO-*d*₆, 100 MHz) δ 156.3 (C-2), 139.5 (C-3), 178.9 (C-4), 161.4 (C-5), 99.8 (C-6), 163.6 (C-7), 95.2 (C-8), 156.7 (C-9), 106.6 (C-10), 130.4 (C-1'), 128.7 (C-2'/6'), 129.2 (C-3'/5'), 131.7 (C-4'), 100.3 (C-1''), 73.6 (C-2''), 76.9 (C-3''), 70.0 (C-4''), 77.6 (C-5''), 61.1 (C-6''), 60.5 (3-OCH₃). HRESIMS m/z 469.1112 [M+Na]⁺ (calcd for C₂₂H₂₂O₁₀Na, 469.1111) and 447.1295 [M+H]⁺ (calcd for C₂₂H₂₃O₁₀, 447.1291). (Supplementary Materials, Figures S21–S27).

3.4.4. Pinocembrin-7-O-β-D-glucopyranoside (7)

White solid. mp. 137–138 °C (130–132 °C [36]). IR (KBr) ν_{\max} cm⁻¹: 3364, 2925, 2858, 1649, 1579, 1296, 1184, 1080. UV (MeOH) λ_{\max} : 285 (2.20), 331 (0.42) nm. ¹H-NMR (DMSO-*d*₆, 400 MHz) δ 12.03 (1H, s, 5-OH), 5.65 (1H, dd, *J* = 2.9, 12.5 Hz, H-2), 3.35 (1H, m, H-3a), 2.85 (1H, dd, *J* = 2.9, 17.2 Hz, H-3b), 6.15 (1H, d, *J* = 2.2 Hz, H-6), 6.20 (1H, d, *J* = 2.2 Hz, H-8), 7.50–7.56 (2H, m, H-2'/6'), 7.36–7.48 (3H, m, H-3'/4'/5'), 4.98 (1H, d, *J* = 7.4 Hz, H-1''), 3.22 (1H, m, H-2''), 3.28 (1H, m, H-3''), 3.15 (1H, m, H-4''), 3.39 (1H, m, H-5''), 3.67 (1H, dd, *J* = 5.2, 11.1 Hz, H-6''a), 3.45 (1H, m, H-6''b), 5.35 (1H, d, *J* = 4.9 Hz, 2''-OH), 5.09 (1H, d, *J* = 4.8 Hz, 3''-OH), 5.02 (1H, d, *J* = 5.2 Hz, 4''-OH), 4.55 (1H, t, *J* = 5.2 Hz, 6''-OH). ¹³C-NMR (DMSO-*d*₆, 100 MHz) δ 79.1 (C-2), 42.7 (C-3), 197.3 (C-4), 163.4 (C-5), 97.1 (C-6), 165.8 (C-7), 96.0 (C-8), 163.0 (C-9), 103.8 (C-10), 138.9 (C-1'), 127.2 (C-2'/6'), 129.1 (C-3'/5'), 129.1 (C-4'), 100.1 (C-1''), 73.5 (C-2''), 76.8 (C-3''), 70.0 (C-4''), 77.6 (C-5''), 61.1 (C-6''). HRESIMS m/z 441.1162 [M+Na]⁺ (calcd for C₂₁H₂₂O₉Na, 441.1162). (Supplementary Materials, Figures S28–S33).

3.5. Biotransformation of 1 by *A. coerulea* KCTC 6936

Scale-up fermentation was carried out under the same process using a modified Czapek Dox medium composed of dextrose (10 g/L), sodium nitrate (2 g/L), dipotassium phosphate (1 g/L), magnesium sulphate (0.5 g/L), potassium chloride (0.5 g/L), and ferrous sulphate (0.02 g/L). Galangin (24 mg, 0.089 mmol) dissolved in DMSO was evenly distributed into four 500 mL Erlenmeyer flasks. After incubation for five days, the culture broth was extracted with EtOAc (0.6 L) four times, and the EtOAc layers were combined

and concentrated under vacuum. The EtOAc extract (55 mg) was chromatographed using Sephadex LH-20 eluted with methanol to give four fractions. Fractions 2 and 3 were further subjected to HPLC using Zorbax SB-CN column (9.4 × 250 mm, Agilent, Santa Clara, CA, USA) with 80% methanol as mobile phase at 2 mL/min to afford galangin-7-*O*-sulfate (4.5 mg, 14.5%).

Galangin-7-*O*-sulfate (8)

Yellow amorphous powder. IR (KBr) ν_{\max} cm^{-1} : 3224, 1635, 1603, 1257, 1218, 1168, 1023, 829. UV (MeOH) λ_{\max} : 265 (1.43), 310 (0.76), 359 (0.99) nm. $^1\text{H-NMR}$ (DMSO- d_6 , 400 MHz) δ 12.27 (1H, s, 5-OH), 9.81 (1H, s, 3-OH), 6.59 (1H, $J = 1.9$ Hz, H-6), 7.02 (1H, $J = 1.9$ Hz, H-8), 8.21 (2H, m, H-2'/6'), 7.57 (3H, m, H-3'/4'/5'). $^{13}\text{C-NMR}$ (DMSO- d_6 , 100 MHz) δ 146.9 (C-2), 138.0 (C-3), 177.2 (C-4), 160.3 (C-5), 101.9 (C-6), 160.1 (C-7), 98.0 (C-8), 155.9 (C-9), 105.7 (C-10), 131.4 (C-1'), 128.1 (C-2'/6'), 129.1 (C-3'/5'), 130.6 (C-4'). HRESIMS m/z 351.0448 [M+H]⁺ (calcd for C₁₅H₁₁O₈S, 351.0175). (Supplementary Materials, Figures S34–S40).

3.6. Cytotoxic Activity Evaluation

The cytotoxic activities of compounds 1–7 against MCF-7 (human breast adenocarcinoma), A375P (human melanoma), B16F10 (murine melanoma), B16F1 (murine melanoma), and A549 (human lung carcinoma) cancer cell lines were performed using the MTT colorimetric method [56]. Briefly, the cells were grown in 96-well plates at a density of 5–6 × 10³ cells/well. After being cultivated for 24 h, cells were treated with various concentrations of compounds for 24 h (MCF-7 A375P, B16F10, and B16F1) and 48 h (A549). Afterwards, each well was replaced with a 100 μL MTT solution (0.5 mg/mL) and incubated for 4 h. A 100 μL of DMSO solution was added into each well after removing the supernatant. The amount of formazan salt was quantified by measuring the absorbance at 490 nm with a microplate reader (SpectraMax 190; Molecular Devices, Sunnyvale, CA, USA). Demethylzeylasteral (DZ) was used as a positive control and DMSO was used as a negative control in all experiments. The cytotoxic activity of the tested compounds was expressed as a half maximal inhibitory concentration (IC₅₀), and the IC₅₀ values are shown in Table 1.

3.7. Hydrolysis of Compounds 4–8

Compounds 4–7 (1 mg each) dissolved in 1 N HCl using a minimum of methanol were heated for 2 h. After cooling, each mixture was neutralized and extracted with EtOAc, respectively. Evaporation of the water layer yielded sugar, which was identified by TLC (CHCl₃/MeOH/H₂O=13:7:2) in comparison with authentic D-glucose [57]. A total of 2.3 mg of sugar was obtained after the acid hydrolysis of compound 4 (7 mg), and its $^{13}\text{C-NMR}$ was measured using D₂O. $^{13}\text{C-NMR}$ (D₂O, 100 MHz) β -form: δ 95.8 (C-1), 75.8 (C-5), 75.6 (C-3), 74.0 (C-2), 69.5 (C-4), 60.6 (C-6); α -form: δ 92.0 (C-1), 72.7 (C-3), 71.4 (C-2), 71.3 (C-5), 69.5 (C-4), 60.5 (C-6).

Compound 8 (2 mg) was dissolved in MeOH and mixed with 3% HCl at room temperature. After evaporation of MeOH, the aglycone (1) was extracted with EtOAc. The aqueous fraction was treated with BaCl₂, resulting in the formation of a white precipitate [38].

4. Conclusions

In summary, galangin (1), 3-*O*-methylgalangin (2), and pinocembrin (3) were isolated from AOH. The corresponding transformation studies with *M. hiemalis* and *A. coerulea* afforded four glucosylated and one sulfated metabolites 4–8. The compound 3-*O*-methylgalangin-7-*O*- β -D-glucopyranoside (6) has never been reported. Compounds 1–7 were evaluated for their cytotoxic activities against five different cancer cell lines using the MTT assay, with metabolite 6 being the most cytotoxic compound. Moreover, it was observed that the activity of flavonols could be significantly improved after 7-*O*-glucosylation. This study is anticipated to expand the structural diversity of flavonoid glucosides and provide a tool to secure sufficient quantities of 4–7 for biological studies.

Supplementary Materials: The following are available online at <https://www.mdpi.com/article/10.3390/catal11091020/s1>, Figure S1: Chromatogram of AOH extract and fractions on TLC silica gel 60 F₂₅₄ plate, Figure S2: ¹³C-NMR spectrum of D-glucose obtained from hydrolysis of compound 4 (D₂O, 100 MHz), Figure S3: Chromatogram of sugars on TLC silica gel 60 F₂₅₄ plate, Figure S4: ¹H-NMR spectrum of compound 1 (CD₃OD, 400 MHz), Figure S5: ¹H-NMR spectrum of compound 2 (DMSO-*d*₆, 400 MHz), Figure S6: ¹H-NMR spectrum of compound 3 (CD₃OD, 400 MHz), Figure S7: HPLC profiles of compounds 4–7, Figure S8: UV-Vis spectra of compounds 4–7 collected with a photodiode array detector, Figure S9: ¹H-NMR spectrum of compound 4 (DMSO-*d*₆, 400 MHz), Figure S10: ¹³C-NMR spectrum of compound 4 (DMSO-*d*₆, 100 MHz), Figure S11: HSQC spectrum of compound 4 (DMSO-*d*₆, 400 MHz), Figure S12: HMBC spectrum of compound 4 (DMSO-*d*₆, 400 MHz), Figure S13: HRESIMS spectrum of compound 4, Figure S14: IR spectrum of compound 4, Figure S15: ¹H-NMR spectrum of compound 5 (DMSO-*d*₆, 400 MHz), Figure S16: ¹³C-NMR spectrum of compound 5 (DMSO-*d*₆, 100 MHz), Figure S17: HSQC spectrum of compound 5 (DMSO-*d*₆, 400 MHz), Figure S18: HMBC spectrum of compound 5 (DMSO-*d*₆, 400 MHz), Figure S19: HRESIMS spectrum of compound 5, Figure S20: IR spectrum of compound 5, Figure S21: ¹H-NMR spectrum of compound 6 (DMSO-*d*₆, 400 MHz), Figure S22: ¹³C-NMR spectrum of compound 6 (DMSO-*d*₆, 100 MHz), Figure S23: HSQC spectrum of compound 6 (DMSO-*d*₆, 400 MHz), Figure S24: HMBC spectrum of compound 6 (DMSO-*d*₆, 400 MHz), Figure S25: Expanded HMBC spectrum of compound 6 (DMSO-*d*₆, 400 MHz), Figure S26: HRESIMS spectrum of compound 6, Figure S27: IR spectrum of compound 6, Figure S28: ¹H-NMR spectrum of compound 7 (DMSO-*d*₆, 400 MHz), Figure S29: ¹³C-NMR spectrum of compound 7 (DMSO-*d*₆, 100 MHz), Figure S30: HSQC spectrum of compound 7 (DMSO-*d*₆, 400 MHz), Figure S31: HMBC spectrum of compound 7 (DMSO-*d*₆, 400 MHz), Figure S32: HRESIMS spectrum of compound 7, Figure S33: IR spectrum of compound 7, Figure S34: ¹H-NMR spectrum of compound 8 (DMSO-*d*₆, 400 MHz), Figure S35: ¹³C-NMR spectrum of compound 8 (DMSO-*d*₆, 100 MHz), Figure S36: HSQC spectrum of compound 8 (DMSO-*d*₆, 400 MHz), Figure S37: HMBC spectrum of compound 8 (DMSO-*d*₆, 400 MHz), Figure S38: IR spectrum of compound 8, Figure S39: HRESIMS spectrum of compound 8, Figure S40: UV-Vis spectrum of compound 8 collected with a photodiode array detector, Figure S41: TLC chromatogram of galangin transformed by *A. coerulea*.

Author Contributions: Conceptualization, I.-S.L.; data curation, F.H.; formal analysis, F.H.; funding acquisition, F.H.; investigation, F.H., Y.X. and I.-S.L.; methodology, F.H. and I.-S.L.; validation, F.H.; project administration, F.H. and I.-S.L.; resources, F.H. and I.-S.L.; supervision, I.-S.L.; visualization, F.H.; writing—original draft preparation, F.H.; writing—review and editing, I.-S.L. and Y.X. All authors have read and agreed to the published version of the manuscript.

Funding: This research was supported by the Basic Science Research Program through the National Research Foundation of Korea (NRF), funded by the Ministry of Education (NRF-2019R111A1A01059410).

Data Availability Statement: Data sharing is not applicable to this article.

Acknowledgments: The authors are grateful for the NMR experimental supports of the Center for Research Facilities, Chonnam National University, and for the HRESIMS analyses of Korea Basic Science Institute (KBSI).

Conflicts of Interest: The authors declare no conflict of interest.

References

1. Ding, P. *Alpinia officinarum* Hance (Gaoliangjiang, galangal). In *Dietary Chinese Herbs: Chemistry, Pharmacology and Clinical Evidence*; Liu, Y., Wang, Z., Zhang, J., Eds.; Springer: Vienna, Austria, 2015; pp. 61–67.
2. Zhang, J.-Q.; Wang, Y.; Li, H.-L.; Wen, Q.; Yin, H.; Zeng, N.-K.; Lai, W.-Y.; Wei, N.; Cheng, S.-Q.; Kang, S.-L.; et al. Simultaneous quantification of seventeen bioactive components in rhizome and aerial parts of *Alpinia officinarum* Hance using LC-MS/MS. *Anal. Methods* **2015**, *7*, 4919–4926. [[CrossRef](#)]
3. Reid, K.; Wright, V.; Omoregie, S. Anticancer properties of *Alpinia officinarum* (lesser galangal)—A mini review. *Int. J. Adv. Res.* **2016**, *4*, 300–306. [[CrossRef](#)]
4. Leclair, H.M.; Tardif, N.; Paris, A.; Galibert, M.-D.; Corre, S. Role of flavonoids in the prevention of AhR-dependent resistance during treatment with BRAF inhibitors. *Int. J. Mol. Sci.* **2020**, *21*, 5025. [[CrossRef](#)]
5. De Oliveira Júnior, R.G.; Ferraz, C.A.A.; Silva, M.G.; de Lavor, É.M.; Rolim, L.A.; de Lima, J.T.; Fleury, A.; Picot, L.; de Souza Siqueira Quintans, J.; Quintans Júnior, L.J.; et al. Flavonoids: Promising natural products for treatment of skin cancer (melanoma). In *Natural Products and Cancer Drug Discovery*; Badria, F.A., Ed.; IntechOpen: London, UK, 2017; pp. 161–210.

6. Pillai, M.K.; Young, D.J.; Bin, H.; Abdul Majid, H.M. Therapeutic potential of *Alpinia officinarum*. *Mini Rev. Med. Chem.* **2018**, *18*, 1220–1232. [[CrossRef](#)]
7. Jiao, H.; Xu, S.; Fan, C.; Zhang, Q.; Wang, Y. Chromatographic fingerprint analysis and quantitative evaluate the rhizomes of *Alpinia officinarum* Hance (lesser galangal). *J. Chin. Pharm. Sci.* **2019**, *28*, 728–738.
8. Basri, A.M.; Taha, H.; Ahmad, N. A review on the pharmacological activities and phytochemicals of *Alpinia officinarum* (galangal) extracts derived from bioassay-guided fractionation and isolation. *Pharmacogn. Rev.* **2017**, *11*, 43–56.
9. Fang, D.; Xiong, Z.; Xu, J.; Yin, J.; Luo, R. Chemopreventive mechanisms of galangin against hepatocellular carcinoma: A review. *Biomed. Pharmacother.* **2019**, *109*, 2054–2061. [[CrossRef](#)]
10. Devadoss, D.; Ramar, M.; Chinnasamy, A. Galangin, a dietary flavonol inhibits tumor initiation during experimental pulmonary tumorigenesis by modulating xenobiotic enzymes and antioxidant status. *Arch. Pharm. Res.* **2018**, *41*, 265–275. [[CrossRef](#)]
11. Zhang, W.; Tang, B.; Huang, Q.; Hua, Z. Galangin inhibits tumor growth and metastasis of B16F10 melanoma. *J. Cell. Biochem.* **2013**, *114*, 152–161. [[CrossRef](#)]
12. Rasul, A.; Millimouno, F.M.; Eltayb, W.A.; Li, J.; Li, X. Pinocembrin: A novel natural compound with versatile pharmacological and biological activities. *Biomed. Res. Int.* **2013**, *2013*, 379850. [[CrossRef](#)]
13. Shen, X.; Liu, Y.; Luo, X.; Yang, Z. Advances in biosynthesis, pharmacology, and pharmacokinetics of pinocembrin, a promising natural small-molecule drug. *Molecules* **2019**, *24*, 2323. [[CrossRef](#)] [[PubMed](#)]
14. Guo, L.; Chen, X.; Li, L.-N.; Tang, W.; Pan, Y.-T.; Kong, J.-Q. Transcriptome-enabled discovery and functional characterization of enzymes related to (2S)-pinocembrin biosynthesis from *Ornithogalum caudatum* and their application for metabolic engineering. *Microb. Cell Fact.* **2016**, *15*, 1–19. [[CrossRef](#)]
15. Zheng, Y.; Wang, K.; Wu, Y.; Chen, Y.; Chen, X.; Hu, C.W.; Hu, F. Pinocembrin induces ER stress mediated apoptosis and suppresses autophagy in melanoma cells. *Cancer Lett.* **2018**, *431*, 31–42. [[CrossRef](#)]
16. Khodzhaieva, R.S.; Gladkov, E.S.; Kyrychenko, A.; Roshal, A.D. Progress and achievements in glycosylation of flavonoids. *Front. Chem.* **2021**, *9*, 637994. [[CrossRef](#)] [[PubMed](#)]
17. Ara, K.Z.G.; Khan, S.; Kulkarni, T.S.; Pozzo, T.; Karlsson, E.N. Glycoside hydrolases for extraction and modification of polyphenolic antioxidants. In *Advances in Enzyme Biotechnology*; Shukla, P., Pletschke, B.I., Eds.; Springer: New Delhi, India, 2013; pp. 9–21.
18. Makris, D.P.; Rossiter, J.T. Heat-induced, metal-catalyzed oxidative degradation of quercetin and rutin (quercetin 3-O-rhamnosylglucoside) in aqueous model systems. *J. Agric. Food Chem.* **2000**, *48*, 3830–3838. [[CrossRef](#)] [[PubMed](#)]
19. Slámová, K.; Kapešová, J.; Valentová, K. “Sweet flavonoids”: Glycosidase-catalyzed modifications. *Int. J. Mol. Sci.* **2018**, *19*, 2126. [[CrossRef](#)] [[PubMed](#)]
20. Bruyn, F.D.; Brempt, M.V.; Maertens, J.; Bellegem, W.V.; Duchi, D.; Mey, M.D. Metabolic engineering of *Escherichia coli* into a versatile glycosylation platform: Production of bioactive quercetin glycosides. *Microb. Cell Fact.* **2015**, *14*, 138. [[CrossRef](#)]
21. Xu, H.; Li, Z.; Wu, Y.; Luo, D.; Qiu, L.; Xie, J.; Li, X. Advances on synthesis of flavonoid glycosides. *Chin. J. Org. Chem.* **2019**, *39*, 1875–1890. [[CrossRef](#)]
22. Hayes, M.R.; Pietruszka, J. Synthesis of glycosides by glycosynthases. *Molecules* **2017**, *22*, 1434. [[CrossRef](#)]
23. Xu, B.; Liang, G.; Wen, Z.; Hu, Z.; Yuan, J.; Chen, H.; Zhang, L. Synthesis of quercetin glycosides and their α -glucosidase inhibitory activities. *Heterocycles* **2016**, *92*, 1245–1260.
24. Li, Y.F.; Yu, B.; Sun, J.S.; Wang, R.X. Efficient synthesis of baicalin and its analogs. *Tetrahedron Lett.* **2015**, *56*, 3816–3819. [[CrossRef](#)]
25. Cano-Flores, A.; Gómez, J.; Escalona-Torres, I.S.; Velasco-Bejarano, B. Microorganisms as biocatalysts and enzyme sources. In *Microorganism*; Blumenberg, M., Shaaban, M., Elgaml, A., Eds.; IntechOpen: London, UK, 2020.
26. Sordon, S.; Popłoński, J.; Huszcza, E. Microbial glycosylation of flavonoids. *Pol. J. Microbiol.* **2016**, *65*, 137–151. [[CrossRef](#)]
27. Han, F.; Xiao, Y.; Lee, I.-S. Microbial transformation of prenylquercetins by *Mucor hiemalis*. *Molecules* **2020**, *25*, 528. [[CrossRef](#)]
28. Lipkind, G.M.; Shashkov, A.S.; Knirel, Y.A.; Vinogradov, E.V.; Kochetkov, N.K. A computer-assisted structural analysis of regular polysaccharides on the basis of ^{13}C -n.m.r. data. *Carbohydr. Res.* **1988**, *175*, 59–75. [[CrossRef](#)]
29. Jiang, J.; Fang, S.; Xu, C.; Luo, J. Studies on the chemical constituents of *Rourea microphylla* (Hook. et Arn) Planch. *Acta Bot. Sin.* **1990**, *32*, 376–379.
30. Pyo, M.K.; Yun-Choi, H.S.; Kim, Y.K. Isolation of n-butyl- β -D-fructopyranoside from *Gastrodia elata* Blume. *Nat. Prod. Sci.* **2006**, *12*, 101–103.
31. Liu, G.; Sun, L.; Wang, S.; Chen, C.; Guo, T.; Ji, Y.; Li, X.; Huang, G.; Wei, H.; Dai, Y.; et al. Hydroxylation modification and free radical scavenging activity of puerarin-7-O-fructoside. *Folia Microbiol.* **2011**, *56*, 305–311. [[CrossRef](#)]
32. Esaki, S.; Abe, M.; Shiba, N.; Kamiya, S. Synthesis of glycyphyllin. *Agric. Biol. Chem.* **1990**, *54*, 1583–1585.
33. Zapesochnaya, G.G. *Datisca cannabina* flavonoids. VII. Galanginin—a new glycoside of galangin. *Khim. Prir. Soedin.* **1982**, *5*, 651.
34. Antri, A.E.; Messouri, I.; Tlemçani, R.C.; Bouktaib, M.; El Alami, R.; El Bali, B.; Lachkar, M. Flavone glycosides from *Calycotome villosa* Subsp. *Intermedia Mol.* **2004**, *9*, 568–573. [[CrossRef](#)]
35. Yang, X.; Zhao, J.; Guo, J.; Mei, S.; Li, L. Flavone compounds isolated from *Lagotis Yunnanensis*. *Chin. Tradit. Herb. Drugs* **2004**, *35*, 257–259.
36. Feng, H.; Wang, Z.; Dong, G.; Wu, Z. Studies on chemical constituents from *Penthorum chinense* Pursh. *Zhongguo Zhongyao Zazhi* **2001**, *26*, 260–262.

37. Varin, L. Flavonoid sulfation: Phytochemistry, enzymology and molecular biology. In *Phenolic Metabolism in Plants. Recent Advances in Phytochemistry*; Stafford, H.A., Ibrahim, R.K., Eds.; Plenum Press: New York, NY, USA; Springer: Boston, MA, USA, 1992; Volume 26, pp. 233–254.
38. Ibrahim, A.R.S. Sulfation of naringenin by *Cunninghamella elegans*. *Phytochemistry* **2000**, *53*, 209–212. [[CrossRef](#)]
39. Teles, Y.C.F.; Souza, M.S.R.; de Souza, M.F.V. Sulphated flavonoids: Biosynthesis, structures, and biological activities. *Molecules* **2018**, *23*, 480. [[CrossRef](#)]
40. Han, F.; Xiao, Y.; Lee, I.-S. Microbial conjugation studies of licochalcones and xanthohumol. *Int. J. Mol. Sci.* **2021**, *22*, 6893. [[CrossRef](#)]
41. Enerstvedt, K.H.; Jordheim, M.; Andersen, Ø.M. Isolation and identification of flavonoids found in *Zostera marina* collected in Norwegian coastal waters. *Am. J. Plant. Sci.* **2016**, *7*, 1163–1172. [[CrossRef](#)]
42. An, N.; Yang, S.; Zou, Z.; Xu, L. Flavonoids of *Alpinia officinarum*. *Chin. Tradit. Herb Drugs* **2006**, *37*, 663–664.
43. Goodarzi, S.; Tabatabaei, M.J.; Jafari, R.M.; Shemirani, F.; Tavakoli, S.; Mofasseri, M.; Tofighi, Z. *Cuminum cyminum* fruits as source of luteolin-7-*O*-glucoside, potent cytotoxic flavonoid against breast cancer cell lines. *Nat. Prod. Res.* **2020**, *34*, 1602–1606. [[CrossRef](#)] [[PubMed](#)]
44. Smiljkovic, M.; Stanisavljevic, D.; Stojkovic, D.; Petrovic, I.; Vicentic, J.M.; Popovic, J.; Grdadolnik, S.G.; Markovic, D.; Sankovic-Babice, S.; Glamoclija, J.; et al. Apigenin-7-*O*-glucoside versus apigenin: Insight into the modes of anticandidal and cytotoxic actions. *Excli J.* **2017**, *16*, 795–807. [[PubMed](#)]
45. Ikemoto, S.; Sugimura, K.; Yoshida, N.; Yasumoto, R.; Wada, S.; Yamamoto, K.; Kishimoto, T. Antitumor effects of *Scutellariae radix* and its components baicalein, baicalin, wogonin on bladder cancer cell lines. *Urology* **2000**, *55*, 951–955. [[CrossRef](#)]
46. Aisyah, L.S.; Yun, Y.F.; Herlina, T.; Julaeaha, E.; Zainuddin, A.; Nurfarida, I.; Hidayat, A.T.; Supratman, U.; Shiono, Y. Flavonoid compounds from the leaves of *Kalanchoe prolifera* and their cytotoxic activity against P-388 murine leukemia cells. *Nat. Prod. Sci.* **2017**, *23*, 139–145. [[CrossRef](#)]
47. Jing, N.; Song, J.; Liu, Z.; Wang, L.; Jiang, G. Glycosylation of anthocyanins enhances the apoptosis of colon cancer cells by handicapping energy metabolism. *BMC Complement. Med. Ther.* **2020**, *20*, 312. [[CrossRef](#)]
48. Zou, T.B.; Feng, D.; Song, G.; Li, H.W.; Tang, H.W.; Ling, W.H. The role of sodium-dependent glucose transporter 1 and glucose transporter 2 in the absorption of cyanidin-3-*O*- β -glucoside in Caco-2 cells. *Nutrients* **2014**, *6*, 4165–4177. [[CrossRef](#)] [[PubMed](#)]
49. Walton, M.C.; McGhie, T.K.; Reynolds, G.W.; Hendriks, W.H. The flavonol quercetin-3-glucoside inhibits cyanidin-3-glucoside absorption in vitro. *J. Agric. Food Chem.* **2006**, *54*, 4913–4920. [[CrossRef](#)] [[PubMed](#)]
50. Medina, R.A.; Owen, G.I. Glucose transporters: Expression, regulation and cancer. *Biol. Res.* **2002**, *35*, 9–26. [[CrossRef](#)]
51. Laudański, P.; Swiatecka, J.; Kovalchuk, O.; Wołczyński, S. Expression of GLUT1 gene in breast cancer cell lines MCF-7 and MDA-MB-231. *Ginekol. Pol.* **2003**, *74*, 782–785.
52. Koch, A.; Lang, S.A.; Wild, P.J.; Gantner, S.; Mahli, A.; Spanier, G.; Berneburg, M.; Müller, M.; Bosserhoff, A.K.; Hellerbrand, C. Glucose transporter isoform 1 expression enhances metastasis of malignant melanoma cells. *Oncotarget* **2015**, *6*, 32748–32760. [[CrossRef](#)] [[PubMed](#)]
53. Xiao, J. Dietary flavonoid aglycones and their glycosides: Which show better biological significance? *Crit. Rev. Food Sci. Nutr.* **2017**, *57*, 1874–1905. [[CrossRef](#)]
54. Srivastava, J.K.; Gupta, S. Extraction, characterization, stability and biological activity of flavonoids isolated from chamomile flowers. *Mol. Cell Pharmacol.* **2009**, *1*, 138–147. [[CrossRef](#)]
55. Amador, S.; Nieto-Camacho, A.; Ramírez-Apan, M.T.; Martínez, M.; Maldonado, E. Cytotoxic, anti-inflammatory, and α -glucosidase inhibitory effects of flavonoids from *Lippia graveolens* (Mexican oregano). *Med. Chem. Res.* **2020**, *29*, 1497–1506. [[CrossRef](#)]
56. Mosmann, T. Rapid colorimetric assay for cellular growth and survival: Application to proliferation and cytotoxicity assays. *J. Immunol. Methods* **1983**, *65*, 55–63. [[CrossRef](#)]
57. Han, F.; Lee, I.-S. A new flavonol glycoside from the aerial parts of *Epimedium koreanum* Nakai. *Nat. Prod. Res.* **2017**, *33*, 320–325. [[CrossRef](#)] [[PubMed](#)]